Modeling of the oxy-combustion calciner in the post-combustion calcium looping process

Jaakko Ylätalo[a]*, Jarno Parkkinen[a], Jouni Ritvanen[a], Tero Tynjälä[a], Timo Hyppänen[a]

[a]*Lappeenranta University of Technology, LUT Energy, P.O. Box 20, 53851 Lappeenranta Finland*

Abstract

The calcium looping process is a fast-developing post-combustion CO_2 capture technology in which combustion flue gases are treated in two interconnected fluidized beds. CO_2 is absorbed from the flue gases with calcium oxide in the carbonator operating at 650 ºC. The resulting $CaCO_3$ product is regenerated into CaO and CO_2 in the calciner producing a pure stream of CO_2. In order to produce a suitable gas stream for CO_2 compression, oxy-combustion of a fuel, such as coal, is required to keep the temperature of the calciner within the optimal operation range of 880-920°C. Studies have shown that the calcium looping process CO_2 capture efficiencies are between 70 % and 97 %. The calciner reactor is a critical component in the calcium looping process. The operation of the calciner determines the purity of gases entering the CO_2 compression. The optimal design of the calciner will lower the expenses of the calcium looping process significantly. Achieving full calcination at the lowest possible temperature reduces the cost of oxygen and fuel consumption. In this work, a 1.7 MW pilot plant calciner was studied with two modeling approaches: 3-D calciner model and 1-D process model. The 3-D model solves fundamental balance equations for a fluidized bed reactor operating under steady-state condition by applying the control volume method. In addition to the balance equations, semi-empirical models are used to describe chemical reactions, solid entrainment and heat transfer to reduce computation effort. The input values of the 3-D-model were adjusted based on the 1-D-model results, in order to model the behavior of the carbonator reactor realistically. Both models indicated that the calcination is very fast in oxy-fuel conditions when the appropriate temperature conditions are met. The 3-D model was used to study the sulfur capture mechanisms in the oxy-fired calciner. As expected, very high sulfur capture efficiency was achieved. After confirming that the 1-D model with simplified descriptions for the sorbent reactions produces similar results to the more detailed 3-D model, the 1-D model was used to simulate calcium looping process with different recirculation ratios to find an optimal area where the fuel consumption is low and the capture efficiency is sufficiently high. It was confirmed that a large fraction of the solids can be recirculated to both reactors to achieve savings in fuel and oxygen consumption before the capture efficiency is affected in the pilot unit. With low recirculation ratios the temperature difference between the reactors becomes too low for the cyclic carbonation and calcination. As a general observation, the small particle size creates high solid fluxes in the calcium looping process that should be taken into account in the design of the system.

Keywords: calcium looping process; calciner; 3-D modeling; 1-D modeling; CO_2 capture; fluidized bed reactor

1. Introduction

Carbon dioxide emissions from stationary sources like power plants burning fossil fuels have been acknowledged to be a contributor to the greenhouse gas phenomenon causing global warming. Carbon dioxide capture and storage (CCS) has emerged as an option to provide a partial solution to this problem [1]. Oxy-fuel combustion and post-combustion solvent techniques have been tested and demonstrated in various pilot scale units [2]. However, the need for more efficient and environmental friendly CCS techniques is a pressing issue [3, 4]. The concept of the post-combustion calcium looping has already been proved at the laboratory scale and now testing on larger scale is being implemented [5, 6]. In post-combustion calcium looping the CO_2 from flue gases is separated with two-interconnected fluidized beds. In the carbonator calcium oxide reacts with carbon dioxide from the flue gases at 650 ºC forming calcium carbonate. After carbonation calcium carbonate is transferred to the calciner where it calcines around 900 ºC to regenerate calcium oxide and a CO_2 flow suitable for transport and storage. Several models have been created and validated for the calcium looping carbonator however little interest has been paid to the calciner [7, 8, 9, 10]. In this work, two modeling approaches are used to study the calciner of a calcium looping process, namely, the 1-D dynamic process model [11] and the 3-D steady-state calciner model. In the 1-D model the full calcium looping process including two interconnected fluidized bed reactors is simulated (Figure 1) albeit with some

* Corresponding author. Tel.: +358-5-62-111; fax: +358-5-621-2498.
E-mail address: jaakko.ylatalo@lut.fi.

simplifying assumptions, such as: no sulfur capture, no make-up flow, no ash accumulation and a uniform particle size. The use of the 1-D approximation and other simplifications for the selected case are justified by carrying out more detailed 3-D simulations for the calciner of the same case. After the validation based on the 3-D model, the 1-D process model is used to study the control of solid circulation between the reactors, and the optimal operation conditions based on capture efficiency and thermal power have been found for the selected cases. The 1.7 MW pilot unit built in Spain is used as the reference case for the simulations [6].

New features of the 1-D model have been described in section 2. The main differences between the 1-D and 3-D models are described in Section 3. In the section 4.1 the results of the 1-D and 3-D simulations are compared and in section 4.2, the hydrodynamics and operation of the calcium looping process can be studied using developed 1-D model. The results show clearly that the efficiency of the process is greatly influenced by the process hydrodynamics. In order to achieve the optimal operation conditions for the complicated dual fluidized bed system, effective solid control systems are needed. This is one of the first attempts to model the whole calcium looping process using a 1-D method, including all key reactions dealing with carbon capture and oxy-fuel combustion. Additionally, the calciner reactor has not been studied with such a detailed model as the 3-D model used in this work. After the experimental validation the developed models will be useful tools in the scale-up studies of the calcium looping process.

2. One-dimensional calciner model

2.1. Model frame

The one-dimensional model frame for the circulating fluidized bed reactor is similar to that presented in previous work [11]. Each reactor is discretized using the control volume method into vertical 1-D control volumes. Spatial derivatives are discretized using first order approximations with central difference or upwind scheme for convective fluxes. Time dependent balance equations for mass and energy are written for each element. A set of time dependent equations is solved using the fixed-step explicit ordinary differential equation solver in Simulink/Matlab system.The major difference between the carbonator and the calciner models is the description of chemical reactions, for mainly combustion. The calciner acts as an oxy-fuel combustor with the purpose of converting $CaCO_3$ to CaO. Following sections describe the additions to the existing model frame.

2.2. Calcination

The accurate description of the calcination reaction is crucial for the model accuracy. Calcination in fluidized bed conditions is widely discussed in literature and several reaction rate models exist [12-17]. For this model a reaction rate equation presented by Fang et al. has been selected [18]. The kinetic coefficient k_{calc} measured by Fang et al. with TGA experiments was used. Calcination in the calcium looping process is generally considered to be a fast chemically controlled reaction if the particles have an average diameter less than 2 mm and the equilibrium condition is met in the oxy-fuel carbon dioxide atmosphere [19]. Careful experimentation has also demonstrated that the Ca-particle size tends to approach 90-100 μm in the cyclic calcium looping conditions [20]. The reaction rate for the calcinations is calculated from the following equation

$$r_{calc} = k_{calc}(1-X)^{2/3}\left(C_{CO2,eq} - C_{CO2}\right) \qquad (1)$$

where r_{calc} is the reaction rate [1/s], (1-*X*) represents the molar fraction of $CaCO_3$ in the solids [-], k_{calc} is the kinetic constant for the calcination reaction [kmol/m^3 s], $C_{CO2,eq}$ is the equilibrium carbon dioxide molar concentration [kmol/m^3] calculated from Equation (2) presented by Silcox et al. [13] and C_{CO2} is the molar concentration of carbon dioxide [kmol/m^3].

$$C_{CO2,eq} = 4.137 \cdot 10^7 \exp\left(\frac{-20474}{T}\right)\frac{m_g}{M_{CO2}V_g} \qquad (2)$$

where m_g is the mass of gas in the element [kg], M_{CO2} molar mass of CO_2 [kg/kmol] and V_g is the volume of gas in the element [m^3].

2.3. Solid fuel combustion model

Solid fuel combustion in the calciner is modeled by dividing the fuel into two reacting components namely char and volatiles, with the amounts of both determined based on the laboratory analysis of the fuel. In the 1-D model the ash and sulfur capture from the fuel and flue gases are not modeled. In reality however, there is a constant make-up flow of fresh calcium carbonate and a purge flow of ash and spent sorbent to avoid the ash and calcium sulfate accumulation in the process. The effect of ash, sulfur and other materials on the reactivity can be taken into account by adjusting the maximum conversion degree of the solid material, as presented by Rodriguez et al. [21]. Sulfur capture in the calciner can be studied in more detail using the 3-D model presented in section 3. The moisture from the fuel is added to the H_2O gas profile and the corresponding latent energy required is removed from the energy equation. In the studied case drying is assumed to be instantaneous, although the model allows also the addition of a moisture release profile. After dividing the inserted fuel into char and volatiles, solid density profile for the char will be defined similarly as for other solid materials [11, 22]. A general reaction rate equation can be written for the char burning [23].

$$r_{char} = k_{char} p_{O2,eff}^{n} \quad (3)$$

where r_{char} is the char reaction rate [1/s], k_{char} is the kinetic coefficient for the combustible fuel [1/Pa s], n is the reaction order of the char [-] and $p_{O2,eff}$ is the effective partial pressure of oxygen [Pa].

$$p_{O2,eff} = \theta p_{O2} \quad (4)$$

where θ [-] is a coefficient that can be used to describe the actual partial pressure of oxygen a char particle experiences in the fluidized bed. The value for the coefficient used in this study is 0.5. The kinetic coefficient varies between fuels; in this case a value for the bituminous coal is used and reaction order n is set to 1 [23]

$$k_{char} = \frac{6}{d_{p,fuel}\rho_{fuel}} 2.092 e^{\frac{-10300}{T}} \quad (5)$$

where $d_{p,fuel}$ is the average fuel particle size [m], ρ_{fuel} is the char particle density [kg/m^3] and T is the temperature of the particle [K]. Average fuel particle size for this study is 500 µm and the char particle density 500 kg/m^3. Fuel char combustion is considered to be a kinetically controlled reaction to keep the modeling approach simple. Char particles are considered spherical and homogeneous without a temperature gradient.

The chemical reactions occurring in char combustion in this model are the following

$C + (1\text{-}2\gamma_{char})O_2 \rightarrow \gamma_{char}CO + (1\text{-}\gamma_{char})CO_2$

$S + O_2 \rightarrow SO_2$

$H + 0.25O_2 \rightarrow 0.5H_2O$

$N + 0.5O_2 \rightarrow NO$

The ratio of CO to CO_2 produced from char combustion is defined by the variable γ_{char}, which can have values between 0 and 1. A NO_x-model has not been built for this system yet and all the nitrogen in the char is converted into NO. The heterogeneous reaction approach is kept simple throughout the model in order to keep the variables to minimum. The justification of the simplifying assumptions is verified by comparing the 1-D results with the more complex 3-D model as discussed in section 4.1. Char mass balance in the system is defined as follows

$$\frac{dm_{char}}{dt} = q_{m,fuel}(1 - w_{moist})w_{char} - \sum_{i=1}^{ntot} m_{char} r_{char,i} \quad (6)$$

where $q_{m,\mathrm{fuel}}$ is the fuel mass flow rate to the system [kg/s], w_{moist} is the mass based moisture content of the fuel [-] and w_{char} is the dry mass-fraction of char in the fuel [-].

In the model it is assumed that no unburned char escapes from the calciner. Although the assumption may not be valid in all of the cases it gives good enough approximation in the current level of modeling. As reality is concerned, char will be entrained from the reactor and will affect the gas balances in the system. The basic elements of the fuel given in the ultimate analysis are divided between char and volatiles based on empirical correlations. The parameters of the fuel used in the simulations are presented in Table 1. Volatile compounds are formed in the model based on the element balance.

The homogenous combustion reactions of volatile compounds are the following in this model [24]. The existing model gas profiles were to be updated with the volatile compounds and reaction rate terms were added to the gas balances.

$CO + 0.5O_2 \rightarrow CO_2$

$CH_4 + 2O_2 \rightarrow CO_2 + 2H_2O$

$C_2H_4 + 3O_2 \rightarrow 2CO_2 + 3H2O$

$H_2S + 1.5O_2 \rightarrow SO_2 + H_2O$

$H_2 + 0.5O_2 \rightarrow H_2O$

$NH_3 + 1.25O_2 \rightarrow NO + H_2O$

Reaction rate equations for each homogeneous reaction have been gathered from various sources [24-29]. A general form for the homogeneous reaction rate equations is

$$r_{gas,a} = m_{gas,tot} k_{gas,a} \frac{1}{T^i} C_{gas,a}^l C_{O2}^m C_{gas,b}^n \qquad (7)$$

where $m_{\mathrm{gas,tot}}$ is the total gas mass, $k_{\mathrm{gas,a}}$ is the reacting gas kinetic coefficient [$\mathrm{m^3\ K^i/kmol\ s}$], $C_{\mathrm{gas,a}}$ is the molar concentration of the reacting gas [$\mathrm{kmol/m^3}$], C_{O2} is the oxygen molar concentration [$\mathrm{kmol/m^3}$] and $C_{\mathrm{gas,b}}$ is the molar concentration of a participating gas [$\mathrm{kmol/m^3}$].

The energy equation of the calciner model was updated with the terms generated from the combustion reactions

$$\frac{dU_i}{dt} = \Delta E_{conv,i} + \Delta E_{disp,i} + \sum_y S_{y,i} - \sum_x Q_{x,i} \qquad (8)$$

where ΔE_{conv}, ΔE_{disp}, S_{i} and Q_{i} represent the convective flows of solids and gas mixture, energy dispersion, the energy source from chemical reactions, and heat transfer rates, respectively [11]. Energy sources from the chemical reactions are now

$$\sum S_{y,i} = -\Delta H_{calc} r_{calc} + r_{char} \sum \left(-\Delta H_{char,i} w_{char,i}\right) + \sum \left(-\Delta H_{gas,a} r_{gas,a}\right) \qquad (9)$$

where $-\Delta H_{\mathrm{char,i}}$ represents different reaction enthalpies of heterogeneous char combustion reactions and $-\Delta H_{\mathrm{gas,a}}$ represents different volatile gas reaction enthalpies.

3. Three-dimensional calciner model

3.1. Model frame

The calciner was modeled three-dimensionally with the CFB3D model code [31], which combines fundamental balance equations with empirical correlations. CFB3D has been developed to model industrial scale CFB units, and it can be used as a tool for optimization, trouble-shooting and risk assessment studies [30]. The model frame includes a three-dimensional description of the furnace which is linked to sub-models describing the hot loop

processes of the CFB boiler: separators return legs and possible external heat exchangers. A more detailed description of the model has been presented by Myöhänen and Hyppänen [31]. The general model frame for the calciner studied in this study is illustrated in Figure 2.

In the model, the calculation mesh is structural with hexahedral calculation cells. The furnace is modeled three-dimensionally by applying a control volume method to discretize and solve the various balance equations in a steady state condition. The first order upwind differencing scheme and the Gauss-Seidel method with successive overrelaxation are used to solve the balance equations which include:

- total gas (continuity and momentum),
- total solids,
- fuel reactions and species (moisture, volatiles and char),
- sorbent reactions and species ($CaCO_3$, CaO, $CaSO_4$ and inert),
- homogeneous reactions and gaseous species (O_2, CO_2, H_2O, SO_2, H_2, CH_4, C_2H_4, C_g, H_2S, NO, N_2O, HCN, NH_3, Ar and N_2),
- energy (heat transfer within the gas-solid suspension and to surfaces, temperature field). [31]

3.2. Sorbent reactions

In the calciner model, there are two different feeds of solids, combustible fuel and sorbent. The number of solids is not limited hence the model is capable of calculating cases where several different fuels are used or the calciner include sorbent make-up flow. The sorbent material is divided into four different species: $CaCO_3$, CaO, $CaSO_4$ and inert material.

The sorbent module includes the reaction rate equations for calcination, carbonation, sulfation, direct sulfation and desulfation reactions.

$CaCO_3 \rightarrow CaO + CO_2$

$CaO + CO_2 \rightarrow CaCO_3$

$CaO + SO_2 + 0.5O_2 \rightarrow CaSO_4$

$CaCO_3 + SO_2 + 0.5O_2 \rightarrow CaSO_4 + CO_2$

$CaSO_4 + CO \rightarrow CaO + SO_2 + CO_2$

The calcination rate equation, r_{calc} [1/s], has been defined based on Silcox et al. [13]:

$$r_{calc} = 1.22 \exp\left(-\frac{4026}{T}\right)\left(p_{CO2,eq} - p_{CO2}\right)A_{m,CaCO3}M_{CaCO3} \quad (10)$$

where $A_{m,CaCO3}$ is the specific reaction surface area of $CaCO_3$ [m^2/kg], M_{CaCO3} is the molecular weight of $CaCO_3$ [kg/mol], p_{CO2} is the CO_2 partial pressure [atm] and $p_{CO2,eq}$ is the equilibrium pressure of CO_2 [atm] defined by Silcox et al. [13]:

$$p_{CO2,eq} = 4.137 \cdot 10^7 \exp\left(\frac{-20474}{T}\right) \quad (11)$$

Contrary to the 1-D model, the 3-D model also includes correlations for the sulfur capture. The correlation for the sulfation rate (12) Myöhänen [30] has developed based on studies by Han et al. [32], Mattison and Lyngfelt [33] and Liu et al. [34].

$$r_{sulf} = 0.001 \exp\left(\frac{-2400}{T}\right)\exp\left(-8X_{CaSO4}\right)C_{SO2}C_{O2}A_{m,CaO}M_{CaO} \quad (12)$$

where X_{CaSO4} is the molar fraction of $CaSO_4$, C_{SO2} is the molar concentration of SO_2 [mol/m^3], $A_{m,CaO}$ is the specific reaction surface area of CaO [m^2/kg] and M_{CaO} is the molecular weight of CaO [kg/mol].

The correlation for the direct sulfation (13) based on equation presented by Hu et al. [35], which Myöhänen [30] has modified.

$$r_{dirs} = 0.01\exp\left(\frac{-3031}{T}\right) C_{SO2}^{0.9} C_{CO2}^{-0.75} C_{O2}^{0.001} A_{m,CaCO3} M_{CaCO3} \qquad (13)$$

The CFB3D model includes also desulfation reaction, which reaction rate Myöhänen [30] has solved with following correlation:

$$r_{desu} = 0.005\exp\left(\frac{-10000}{T}\right) C_{CO} A_{m,CaSO4} M_{CaSO4} \qquad (14)$$

where $A_{m,CaSO4}$ is the specific reaction surface area of $CaSO_4$ [m^2/kg] and M_{CaSO4} is the molecular weight of $CaSO_4$ [kg/mol].

The 3-D model was used to study the importance of different sulfur capture mechanisms in the operation conditions of the oxy-fired calciner. In Figure 3, the sulfur concentration within the reactor is shown. Sulfur capture efficiency in the calciner is practically 100 % due to the high Ca/S ratio in the calciner. The formation of calcium sulfate determines the minimum make-up flow needed in the calcium looping process in order to keep the amount of active sorbent sufficient for the CO_2 capture. However, the importance of the exothermic sulfation reactions to the overall energy balance is negligible and the omitting of the sulfur reaction equations from the 1-D model can be justified.

4. Results

The main dimensions of the modeled process correspond to the 1.7 MW calcium looping pilot plant located in Spain [6]. The main operating parameters used in the models are listed in Table 2. The circulation coefficient presented in the Table 2 is an empirical coefficient that depends on the geometry of the exit channel, hydrodynamic regime of the reactor and the reactor aspect ratio (Ylätalo et al. 2012). High value for the circulation coefficient was selected based on knowledge about the high aspect ratio of the reactors and small particle size. The whole process is simulated with the 1-D model whereas in the 3-D model only the calciner is modeled. The simulated solid circulation rate, conversion degree of the solid material and solid temperature acquired from the 1-D carbonator are used in the 3-D calciner as inputs. One reasonable operation point was selected and the operation of the calciner was studied using both models. Simulation results were compared and validity of the models was studied. After that the recirculation of solids was adjusted gradually in the 1-D model in order to find the optimal operation conditions which will minimize the fuel and oxygen consumption of the calciner and still remain at high capture efficiency. Recirculation is the fraction of solids that is transferred back to the same reactor from which they leave. In all of the simulations, both reactors have the same amount of recirculation in order to keep the amount of simulation points at a reasonable level. The same amount of solid material traveling between the reactors could also be achieved by using different combinations of recirculation and fulfilling the mass balance but this option is excluded from this study.

4.1. Comparison of the 1-D and 3-D simulation results for the calciner

In the comparison of the 1-D and 3-D models, the thermal power of the calciner was 1.58 MW, the recirculation percentage 60 % and the carbonator cooling power was 420 kW. Other operation conditions for the studied case are given in Table 2. The calculated solid circulation rate for this case was 4.54 kg/s for the 1-D model and 4.56 kg/s for the 3-D model with 2.9 m/s gas velocity. Solid inventories in the calciner reactors were 259 kg with the 1-D and 262 kg with the 3-D model.

In Figure 4a, the vertical temperature profiles averaged over the calciner cross section calculated with both models are presented. The trend of both reactors is close to each other and the values range between 5-10 ºC which

is acceptable. Small differences in temperature profiles can be explained mainly by the fundamental differences between the models. The 3-D-model which has a more dense calculation mesh takes into account more physical phenomena and more initial variables need to be defined and also some lateral effects are present. In Figure 4b, the 3-D image of the temperature and horizontal temperature gradients can be observed near to the material feed points of the calciner, even though the overall behavior of the reactor can be considered one dimensional. In larger units, the complexity of the 3-D-model is expected to be more useful, demonstrating the effect of local gradients on the whole process. The temperature of the calciner is in the bottom area below calcination conditions because of the cold flow solid coming from the carbonator. At the height of the fuel inlet, however the temperature rises quickly to the calcining conditions.

Figure 5a presents the average vertical profile of the volume fraction of CO_2 in the gases in the 1-D and 3-D simulations and in Figure 5b the 3-D volume fraction of CO_2 in the gases is presented. From the development of the CO_2 profile it can be concluded that the calcination and combustion are very fast when the temperature reaches 890-900 ºC at the current oxy-fuel conditions. Maintaining high enough temperature is the most important factor in achieving full calcination. The vertical CO_2 profiles match quite well indicating that both the 1-D and 3-D models predict similar calcination behavior in these conditions. Some differences can be noticed in the fuel inlet area which can be explained by the simplifications made in the 1-D combustion model.

Figure 6a describes the vertical development of the fraction of $CaCO_3$ in the solids in both models. From the figure it can be concluded that the majority of the calciner reactions occur within the first 3-4 meters from the bottom. The depletion of $CaCO_3$ in the solids demonstrates the speed of the calcination reaction for solids. From the 1-D profile it can be shown that the calcination reaction and strong mixing in the fluidized bed drive the fraction of $CaCO_3$ close to zero, in other words full calcination is achieved. Differences between the models are small, but the gradients in the bottom area are higher in the 1-D model because of the larger control volumes in the vertical direction. In Figure 6b 3-D contours of the $CaCO_3$ concentration are shown. Despite the asymmetry at the bottom where the inlet of $CaCO_3$ from the carbonator is clearly shown, the mixing is very intense and the overall behavior of the studied calciner can be well modeled using a 1-D assumption.

4.2. Effect of hydrodynamics on process efficiency and fuel consumption

After the validation of the 1-D model using the 3-D model results, the 1-D-model was used to simulate ten different recirculation values ranging from no recirculation to all the solid material being recirculated. The system parameters were the same as those previously presented for the 1-D and 3-D comparison case, only here, the thermal power and carbonators cooling were modified. The fuel feed was adjusted to keep the calciner operating at the correct temperature. The oxygen to carbon dioxide molar ratio was kept constant although the need for oxygen decreased when fuel feed decreased. The carbonator reactor was simulated alongside the calciner in order to predict the carbonation conversion and temperature of the solids entering the calciner. Figure 7 presents the capture efficiency of the system, calcination efficiency and the thermal power of the calciner and carbonator cooling power as a function of solid recirculation. With no solid recirculation, achieving a high enough temperature difference between the reactors is difficult even though the fuel feed and carbonator cooling are high. When the recirculation is small the temperature of the calciner is too low and the temperature of the carbonator is too hot for the carbonation conditions. By contrast, with very high recirculation, the amount of active material traveling between reactors is insufficient to capture all the CO_2 from the flue gases. However, it is good to notice that the results presented here apply mainly for the construction used in the studied pilot plant. With a different construction and appropriately designed heat integration of the reactors, it could be possible to operate calcium looping process with good capture efficiency also without solid recirculation. Figure 8 presents the values of solid fluxes out of the reactors in the different cases. It has to be noted that the solid fluxes start to change when the recirculation becomes very high. This is because the gas velocity in the calciner is decreasing due to the lower volumetric gas flow. In the same figure the molar flow of CaO is compared to the molar flow CO_2 arriving to the carbonator. The recirculation is taken into account when calculating the molar flow CaO to the carbonator. It seems that although the flux of CaO the carbonator is high in the no recirculation case, the low calcination rate creates a lack of active CaO in the carbonator which can be seen also in Figure 7. Based on Figure 7 it can be determined that the optimal recirculation ratio in the

studied case is around 60-70 % to achieve over 90 % capture efficiency for this operation point. It has to be noted that the solid circulation rate in the studied case is so high, around 3.0-4.6 kg/s, that the calcination efficiency does not have to be 100 % to achieve good capture efficiencies in the carbonator. Also the linear decrease of fuel feeding and cooling is not the best possible option in this case. With high recirculation ratios the calciner temperature starts rising rapidly but this can be ignored because the capture efficiency is already poor. With lower recirculation values the calcination efficiency could have been raised to 100 % with high thermal power but due to the fact that the practical cooling power is limited the temperature difference between the reactors would still have been too low for the carbonation process to take place. If the economy of the process is to be studied in more detail each point should be optimized case by case to find the lowest fuel consumption to cooling ratio. In addition, the optimal area of the recirculation will change depending on the capture load of the calcium looping process. The point of this exercise was to demonstrate that good solid circulation regulation is crucial in calcium looping in order to keep the process operation at the optimal level. The fine limestone particles lead easily to high solid fluxes in the fast fluidization conditions and there are few options to control the flow. One way is to transfer the operation of the reactors to a different fluidization regime by adjusting the volumetric flow of the fluidizing gas, increasing the reactor size or particle size. Increasing reactor size will impair the process, with growing costs and losses. The particle size is difficult to maintain because of the reasons mentioned earlier in section 2.2. The calciner reactor gas flow and velocity is linked to the carbonator flue gas load which is defined by requirement of CO_2 capture from the boiler. It is important to remember that the flue gas flow will change depending on the boiler load. In the current state, the most reasonable solution is to recirculate part of the solid material back to each reactor in order to reduce the thermal stress of the process and still maintain enough active material traveling between the reactors.

5. Conclusion

This paper discusses the process modeling of the oxy-combustion calciner in the calcium looping process. The oxy-combustion calciner was studied with two modeling approaches: a 1-D dynamic process model and a 3-D steady-state calciner model. A sample calculation case was built based on a 1.7 MW calcium looping pilot plant located in Oviedo, Spain. The selected calculation cases were simulated with both models at steady-state conditions. Both models indicated that the calcination is very fast in oxy-fuel conditions, when the temperature condition is fulfilled. Differences between the model results were very small, which indicates that the behavior of the pilot plant is adequately described by a one dimension model for most situations. However, with larger units, the lateral effects will become more dominant and the 3-D model will give more realistic predictions of the reactor behavior. The 3-D model was used to study the sulfur capture mechanisms in oxy-fired calciner. As expected, very high sulfur capture efficiency was achieved. After confirming that the 1-D model with simplified descriptions for the sorbent reactions produces similar results as more detailed 3-D model, the 1-D model was used to simulate the calcium looping process with different recirculation ratios to find an optimal regime where the fuel consumption is low and the capture efficiency is sufficiently high. It was confirmed that a large fraction of the solids can be recirculated to both reactors to achieve savings in fuel and oxygen consumption before the capture efficiency is affected in the pilot plant. With low recirculation ratios the temperature difference between the reactors becomes too low for the cyclic carbonation and calcination. As a general observation, the small particle size creates high solid fluxes in the calcium looping process that should be taken into account in design of the system.

6. Acknowledgements

The research leading to these results has received funding from the European Community's Seventh Framework Programme (FP7/2007-2013) under GA 241302-CaOling Project.

7. References

[1] Metz B, Davidson O, de Coninck H, Loos M, Meyer L. Special report on carbon dioxide capture and storage. In: Intergovernmental panel on climate change. Cambridge, UK: Cambridge University Press; 2005.

[2] McCauley KJ, Farzan H, Alexander KC, McDonald DK, Varagani R, Prabhakar R, Tranier J-P, Perrin N. Commercialization of oxy-coal combustion: Applying results of a large 30 MWth pilot project. Energy Procedia 2009;1:439-446.

[3] Shimizu T, Hirama T, Hosoda H, Kitano K, Inagaki M, Tejima K. A twin fluid-bed reactor for removal of CO_2 from combustion processes. Chemical Engineering Research and Design 1999;77:62-68.
[4] Anthony EJ. Solid looping cycles: a new technology for coal conversion. Ind Eng Chem Res 2008;47:1747.
[5] Rodriguez N, Alonso M, Abanades JC. Experimental investigation of a circulating fluidized-bed reactor to capture CO_2 with CaO. AIChE Journal 2011;57:1356-1366.
[6] Sánchez-Biezma A, Ballesteros JC, Diaz L, Zárraga E de, Álvarez FJ, López J, Arias B, Grasa G,Abanades JC. Postcombustion CO2 capture with CaO. Status of the technology and next steps towards large scale demonstration. Energy Procedia 2011;4:852-859.
[7] Hawthorne C, Trossmann M, Cifre PG, Schuster A, Scheffknecht G. Simulation of the carbonate looping power cycle. Energy Procedia 2009;1:1387-1394. Greenhouse Gas Control Technologies 9, Proceedings of the 9th International Conference on Greenhouse Gas Control Technologies (GHGT-9), 16-20 November 2008, Washington DC, USA.
[8] Alonso M, Rodriguez N, Grasa G, Abanades JC. Modelling of a fluidized bed carbonator reactor to capture CO_2 from a combustion flue gas. Chemical Engineering Science 2009;64:883-891.
[9] Romano M. Modeling the carbonator of a Ca-looping process for CO_2 capture from power plant flue gas. Chemical Engineering Science 2012;69:257-269.
[10] Lasheras A, Ströhle J, Galloy A, Epple B. Carbonate looping process simulation using a 1D fluidized bed model for the carbonator. International Journal of Greenhouse Gas Control 2011;5:686-693.
[11] Ylätalo J, Ritvanen J, Arias B, Tynjälä T, Hyppänen T. 1-Dimensional modeling and simulation of the calcium looping process. International Journal of Greenhouse Gas Control 2012;9:130-135.
[12] Baker E.H. The calcium oxide-carbon dioxide system in the pressure range of 1-300 atmospheres. Journal of the Chemical Society 1962;70: 464-470.
[13] Silcox G, Kramlich J, Pershing D. A mathematical model for the flash calcination of dispersed $CaCO_3$ and $Ca(OH)_2$ particles. Industrial and Engineering Chemistry Research 1989;28:155–160.
[14] García-Labiano F, Abad A, de Diego L, Gayán P, Adánez J. Calcination of calcium based sorbents at pressure in a broad range of CO_2 concentrations. Chemical Engineering Science 2002;57:2381-2393.
[15] Martínez I, Grasa G, Murillo R, Arias B, Abanades JC. Kinetics of Calcination of Partially Carbonated Particles in a Ca-Looping System for CO_2 Capture. Energy & Fuels 2012;26:1432-1440.
[16] Takkinen S, Saastamoinen J, Hyppänen T. Heat and Mass Transfer in Calcination of Limestone Particles. AIChE Journal 2012;58:2563–2572.
[17] Takkinen S, Hyppänen T, Saastamoinen J, Pikkarainen T. Experimental and Modeling Study of Sulfur Capture by Limestone in Selected Conditions of Air-Fired and Oxy-fuel Circulating Fluidized-Bed Boilers. Energy Fuels 2011;25:2968–2979.
[18] Fang F, Li Z, Cai N. Experiment and Modeling of CO2 Capture from Flue Gases at High Temperature in a Fluidized Bed Reactor with Ca-based Sorbents. Energy & Fuels 2009;23:207-216.
[19] Dennis J, Hayhurst A. The Effect of CO2 on the Kinetics and Extent of Calcination of Limestone and Dolomite Particles in Fluidized beds. Chemical Engineering Science 1987;42:2361-2372
[20] González B, Alonso M, Abanades JC. Sorbent attrition in a carbonation/calcination pilot plant for capturing CO_2 from flue gases. Fuel 2010; 89:2918-2924.
[21] Rodríguez N, Alonso M, Abanades JC. Average activity of CaO particles in a calcium looping system. Chemical Engineering Journal 2010; 156:388-394.
[22] Johnsson F, Leckner B. Vertical distribution of solids in a CFB-furnace, in: K. Heinschel (Ed.), Proceedings of the 13th International Conference on Fluidized Bed combustion. 1995:671-679, Orlando, FL, USA. May 07-10.
[23] Basu P. Combustion and Gasification in Fluidized Beds.2006. ISBN-0849333962
[24] De-Souza Santos M. Solid Fuels Combustion and Gasification. 2010. CRC Press. ISBN-9781420047493
[25] Yetter, R.A., Dryer, F.L., and Rabitz, H. Complications of one-step kinetics for moist CO oxidation. Proc. 21st Symposium (International) on Combustion, Combustion Institute, 1986, pp. 749–760.
[26] Vilienskii, T.V., and Hezmalian, D.M. Dynamics of the combustion of pulverized fuel. Energia (Moscow), 11, 246–251, 1978.
[27] Branch, M.C., and Sawyer, R.F.. Ammonia oxidation kinetics in an arc heated flow reactor. Proc. 14th Symposium (International) on Combustion, Pittsburgh, PA, 1973, pp. 967–974.
[28] Leveson, P.D., Kinetic Studies to Determine the Rates of Ammonia and Hydrogen Sulphide Destruction Under Claus Plant Operating Conditions, PhD thesis, University of Sheffield, Department of Chemical Engineering And Fuel Technology, Sheffield, United Kingdom, 1997.
[29] Quan, V., Marble, F.E., and Klingel, J.R. Proc. 14th Symposium (International) on Combustion, Pittsburgh, PA, August 20–25, 197, pp. 851–60.
[30] Myöhänen K. Modelling of combustion and sorbent reactions in three-dimensional flow enviroment of a circulating fluidized bed furnace. dissertation. 2011. Lappeenranta. ISBN 978-952-265-160-0.
[31] Myöhänen K, Hyppänen T. A Three-Dimensional Model Frame for Modelling Combustion and Gasification in Circulating Fluidized Bed Furnaces. International Journal of Chemical Reactor Engineering 2011; 9: Article A25.
[32] Han K., Lu C., Cheng S., Zhao G., Wang Y., Zhao J. Effect of characteristics of calcium-based sorbents on the sulfation kinetics. Fuel 2005; 84: 1933-1939.
[33] Mattisson T., Lyngfelt A. A sulphur capture model for circulating fluidized-bed boilers. Chemical Engineering Science 1998; 53: 1163-1173.
[34] Liu H., Katagiri S., Kaneko U., Okazaki K. Sulfation behavior of limestone under high CO_2 concetration in O_2/CO_2 coal combustion. Fuel 2000; 79: 945-953.

[35] Hu G., Shang L., Dam-Johansen K., Wedel S., Hansen J.P. Initial kinetics of the direct sulfation of limestone. AIChE 2008;54:2663-2673.

Figure 1. 1-D dynamic model frame for the calcium looping process, including the carbonator and calciner, return leg and cyclones.

Figure 2. 3-D steady-state calciner model frame with the solid circulation system.

Figure 3. 3-D plot of the SO_2 molar percentage in the flue gases of the calciner.

Figure 4a.Vertical temperature profile of the calciner in 1-D and 3-D models.

Figure 4b. The 3-D temperature gradient plot.

Figure 5a. Vertical molar fraction profile of CO_2 in 1-D and 3-D models.

Figure 5b. The 3-D CO_2 molar-fraction in gases.

Figure 6a. Vertical molar fraction profile for $CaCO_3$ in the solids in both models.

Figure 6b. 3-D plot of the molar fraction of $CaCO_3$ in the solids.

Figure 7. Capture and regeneration efficiencies plotted as a function of the recirculation percentage on the left hand side axis. The calciner thermal power and the carbonator cooling as a function of recirculation percentage on the right hand side axis.

Figure 8. Solid flux of the carbonator and calciner plotted as function of recirculation on the left hand side axis. Relation of molar flow CaO to molar flow CO_2 to the carbonator as function of recirculation on the right hand side axis.

Table 1. Properties of the fuel used in the simulations.

Table 2. Input values, simulation parameters and boundary conditions of the models in all of the calculation cases.

Figure 1.

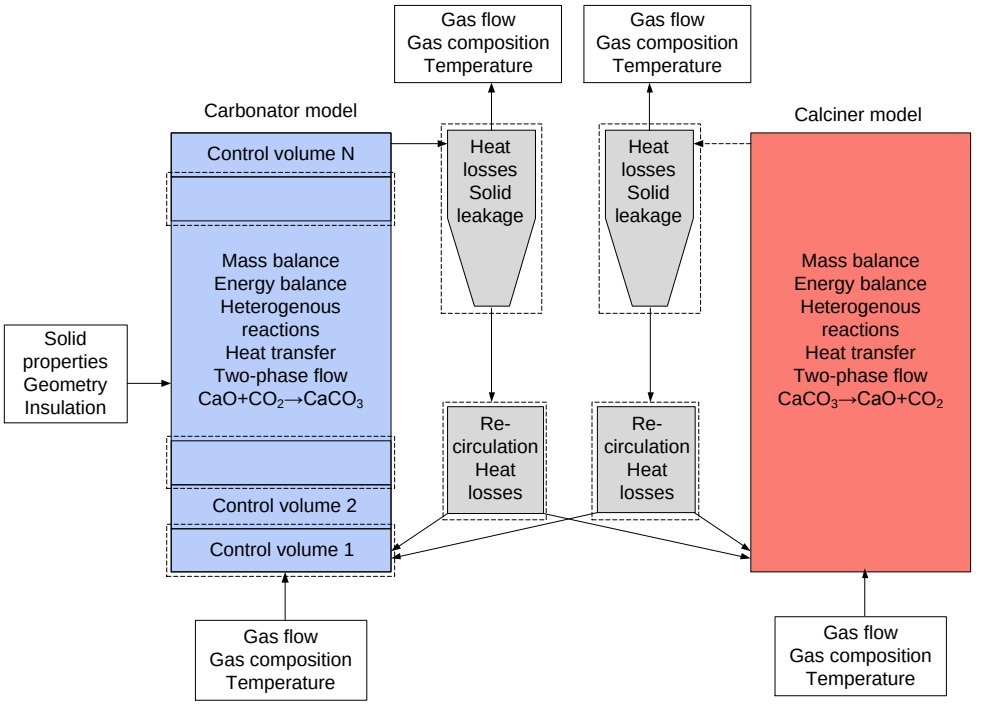
Gas flow
Gas composition
Temperature
Gas flow
Gas composition
Temperature
Carbonator model
Calciner model
Control volume N
Heat losses
Solid leakage
Heat losses
Solid leakage
Mass balance
Energy balance
Heterogenous reactions
Heat transfer
Two-phase flow
CaO+CO2→CaCO3
Solid properties
Geometry
Insulation
Re-circulation
Heat losses
Re-circulation
Heat losses
Mass balance
Energy balance
Heterogenous reactions
Heat transfer
Two-phase flow
CaCO3→CaO+CO2
Control volume 2
Control volume 1
Gas flow
Gas composition
Temperature
Gas flow
Gas composition
Temperature

Figure 2.

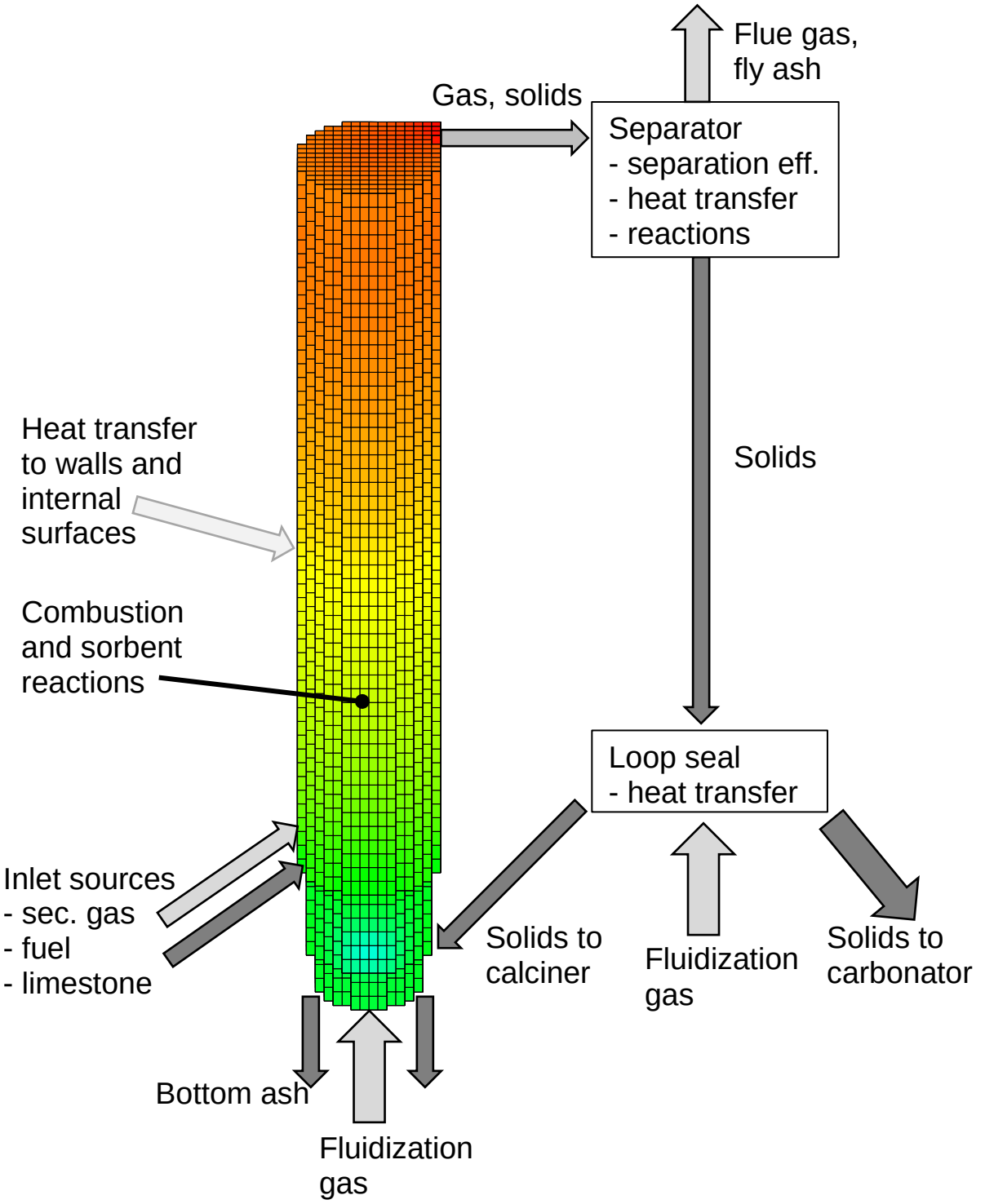
Flue gas,
fly ash
Gas, solids
Separator
- separation eff.
- heat transfer
- reactions
Heat transfer
to walls and
internal
surfaces
Solids
Combustion
and sorbent
reactions
Loop seal
- heat transfer
Inlet sources
- sec. gas
- fuel
- limestone
Solids to
calciner
Fluidization
gas
Solids to
carbonator
Bottom ash
Fluidization
gas

Figure 3.

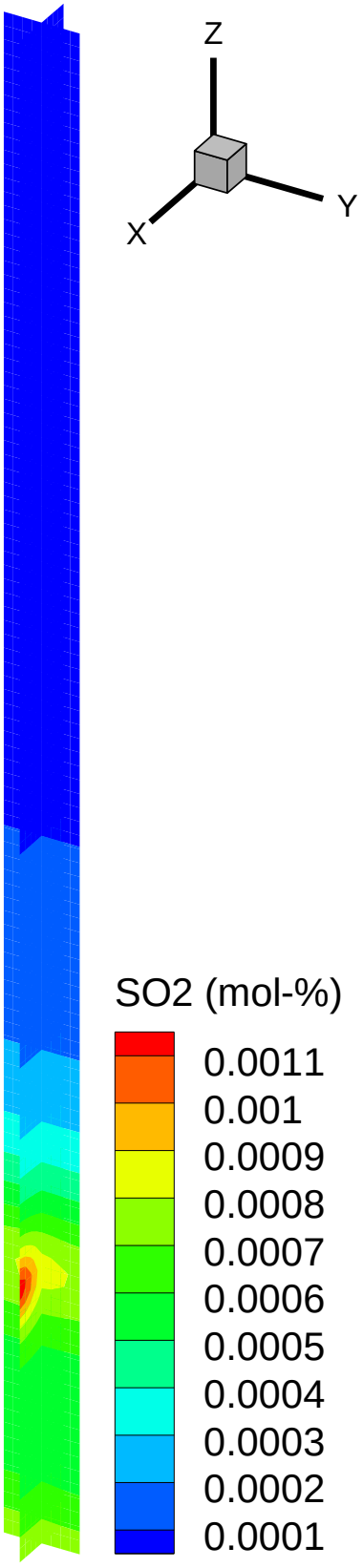
Z
Y
X
SO2 (mol-%)
0.0011
0.001
0.0009
0.0008
0.0007
0.0006
0.0005
0.0004
0.0003
0.0002
0.0001

Figure 4a.

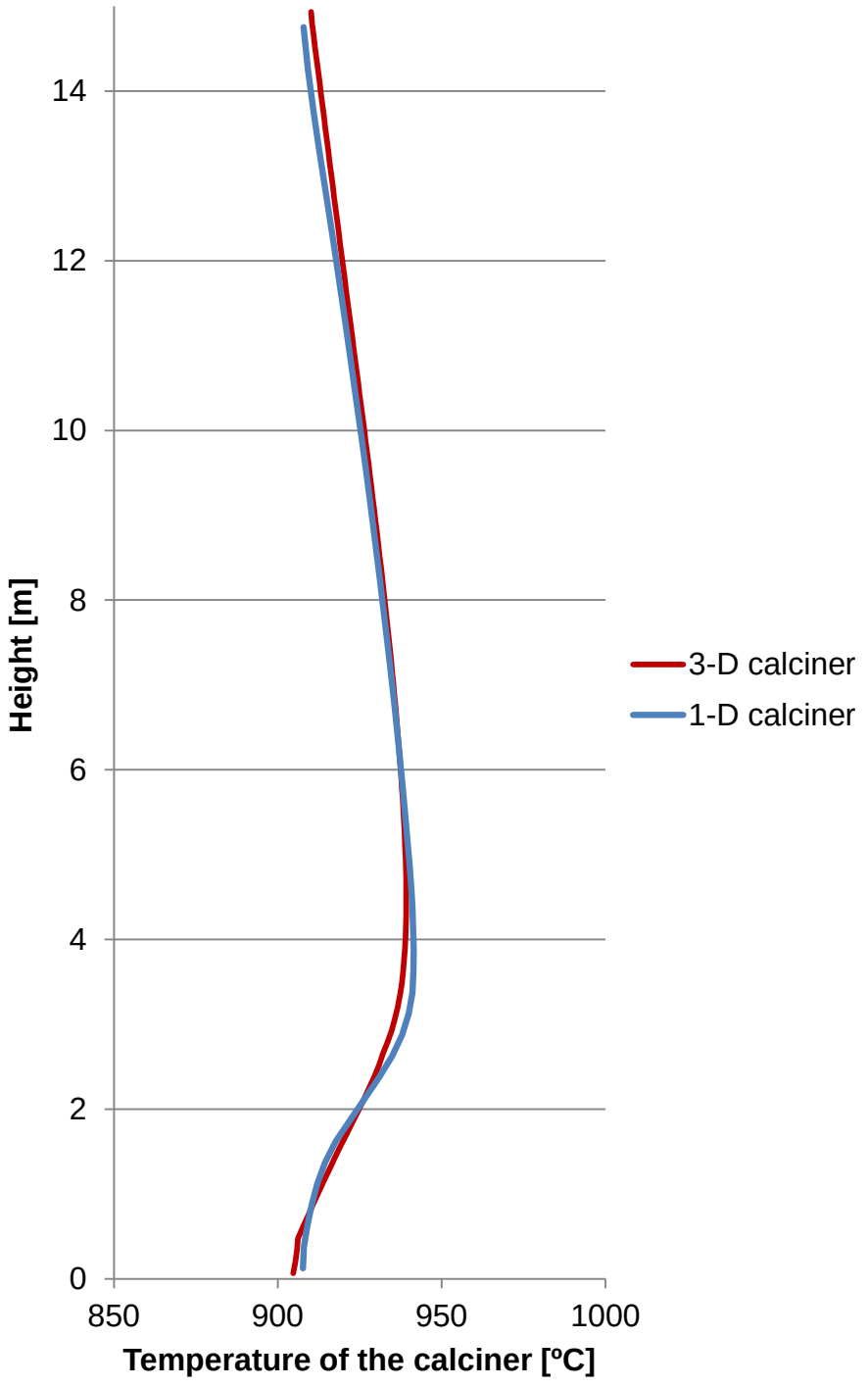
14
12
10
8
6
4
2
0
Height [m]
850
900
950
1000
Temperature of the calciner [ºC]
3-D calciner
1-D calciner

Figure 4b.

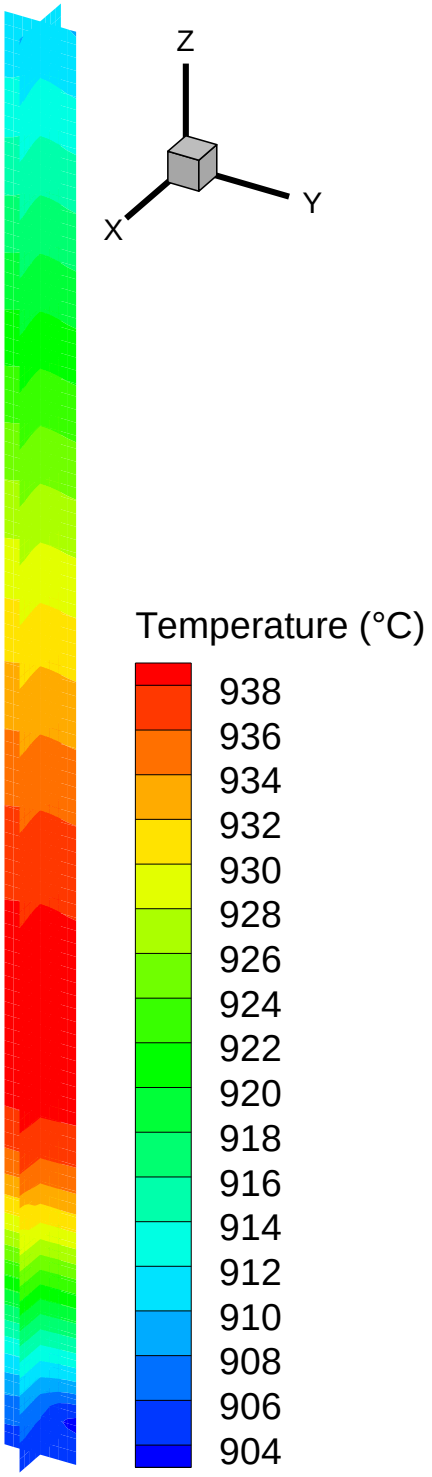
Z
X
Y
Temperature (°C)
938
936
934
932
930
928
926
924
922
920
918
916
914
912
910
908
906
904

Figure 5a.

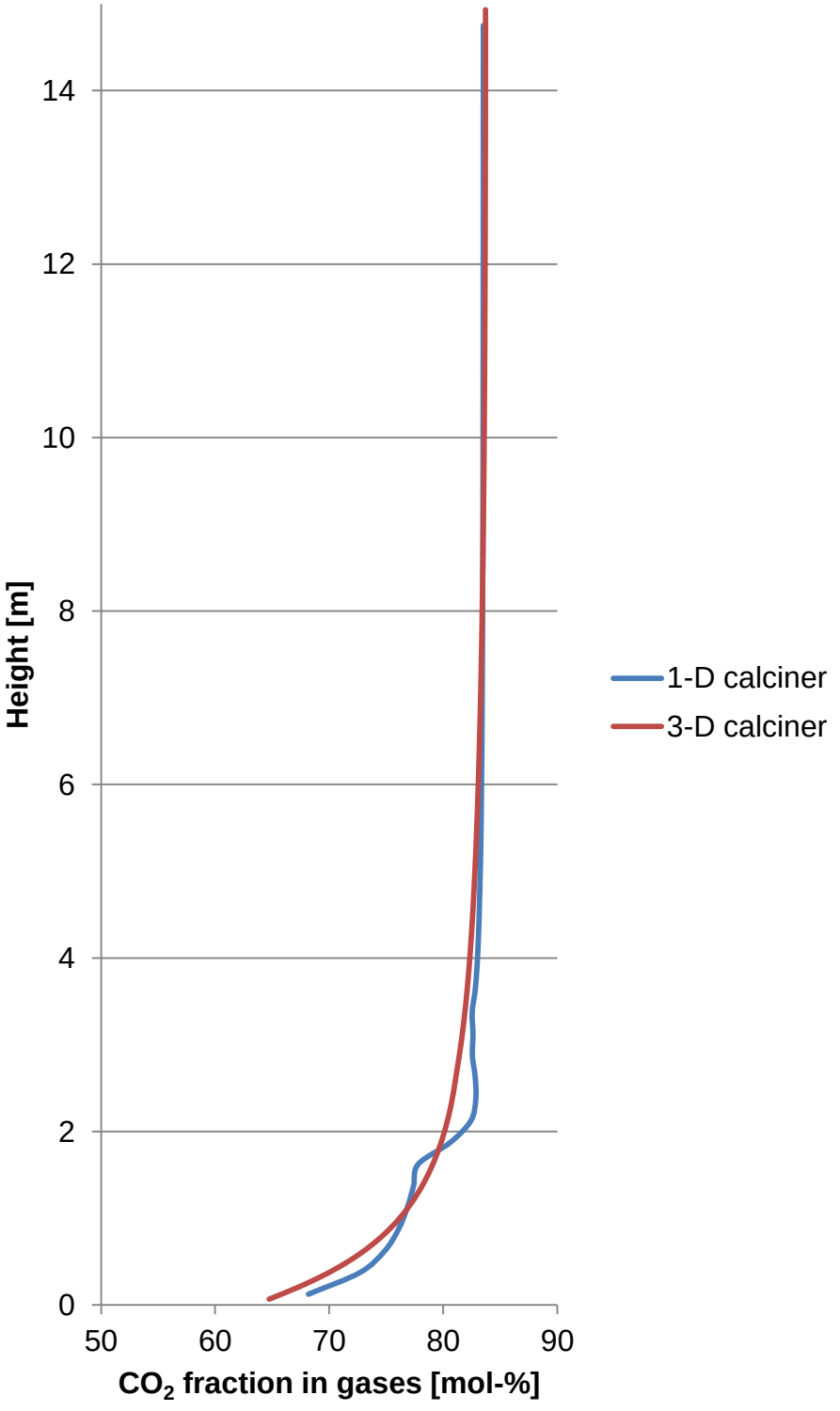
14
12
10
8
6
4
2
0
Height [m]
50
60
70
80
90
CO2 fraction in gases [mol-%]
1-D calciner
3-D calciner

Figure 5b.

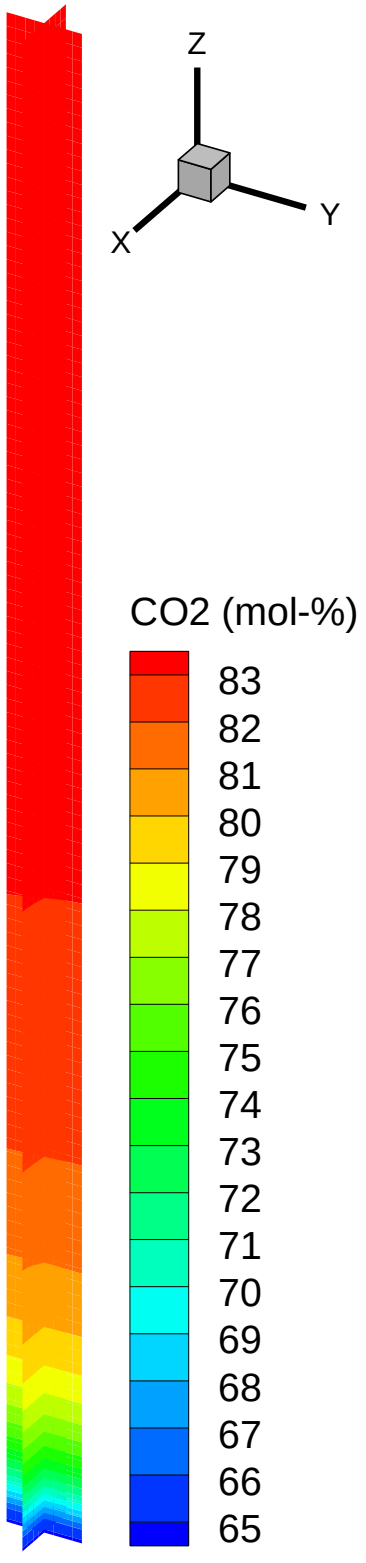

Figure 6a.

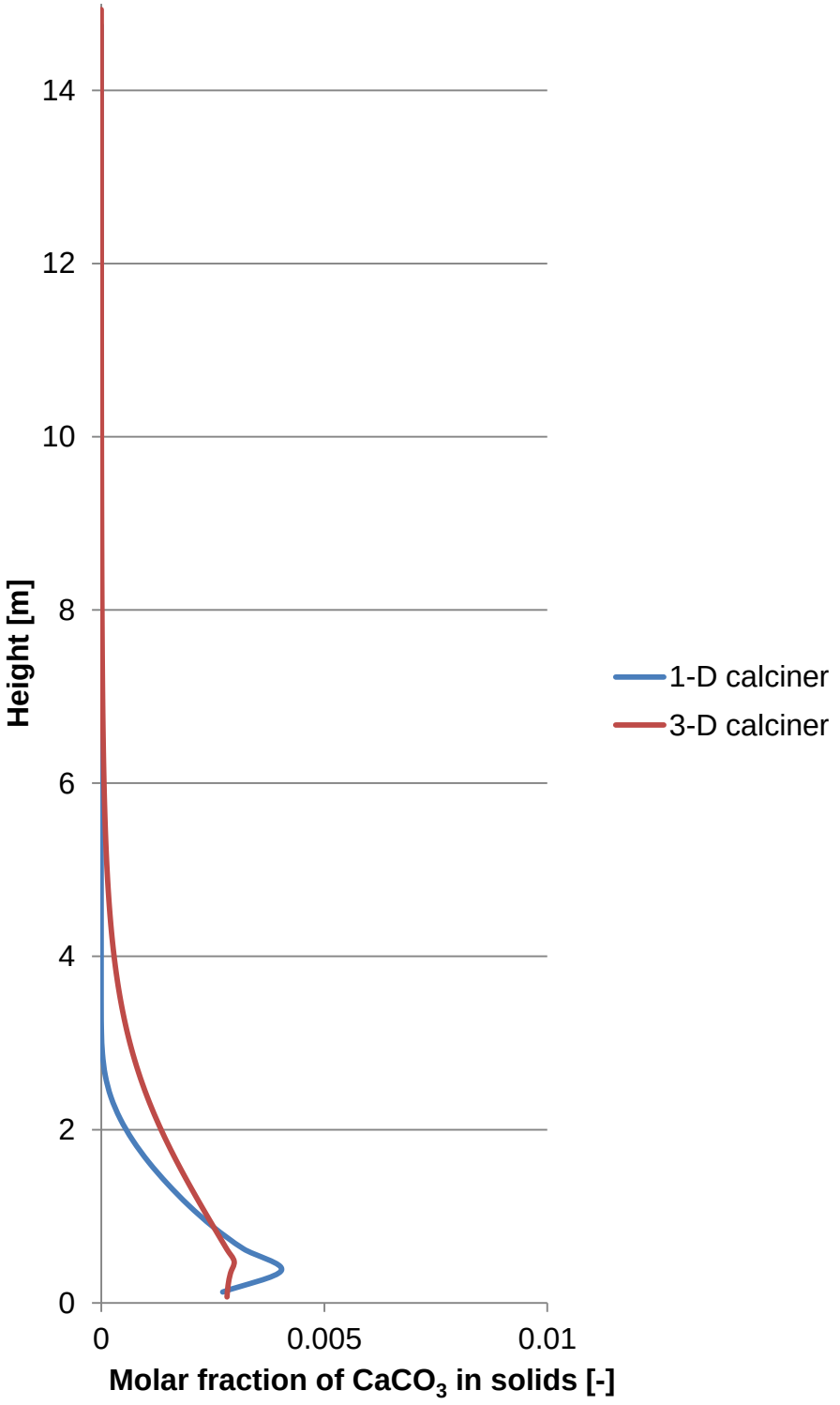
14
12
10
8
6
4
2
0
Height [m]
0
0.005
0.01
Molar fraction of CaCO3 in solids [-]
1-D calciner
3-D calciner

Figure 6b.

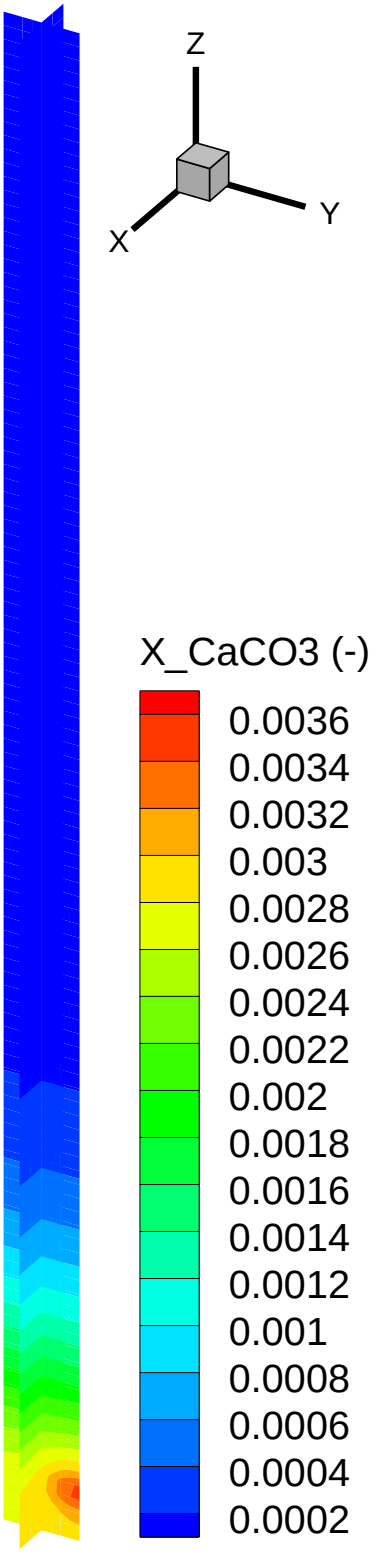
Z
X
Y
X_CaCO3 (-)
0.0036
0.0034
0.0032
0.003
0.0028
0.0026
0.0024
0.0022
0.002
0.0018
0.0016
0.0014
0.0012
0.001
0.0008
0.0006
0.0004
0.0002

Figure 7.

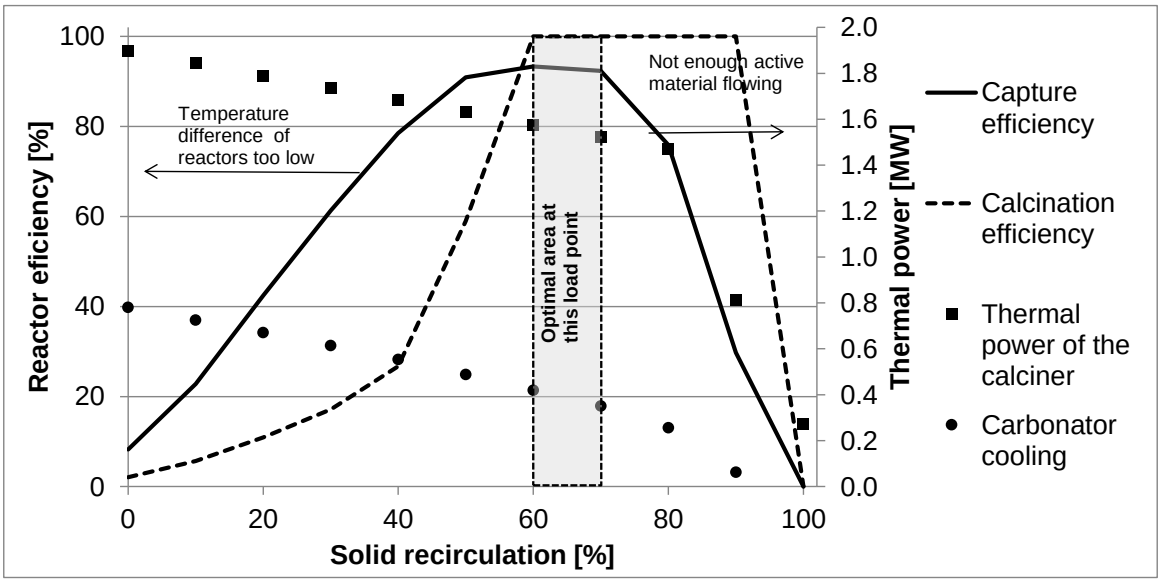
Reactor eficiency [%]
Thermal power [MW]
Solid recirculation [%]
Temperature difference of reactors too low
Not enough active material flowing
Optimal area at this load point
Capture efficiency
Calcination efficiency
Thermal power of the calciner
Carbonator cooling
0
20
40
60
80
100
0.0
0.2
0.4
0.6
0.8
1.0
1.2
1.4
1.6
1.8
2.0

Figure 8.

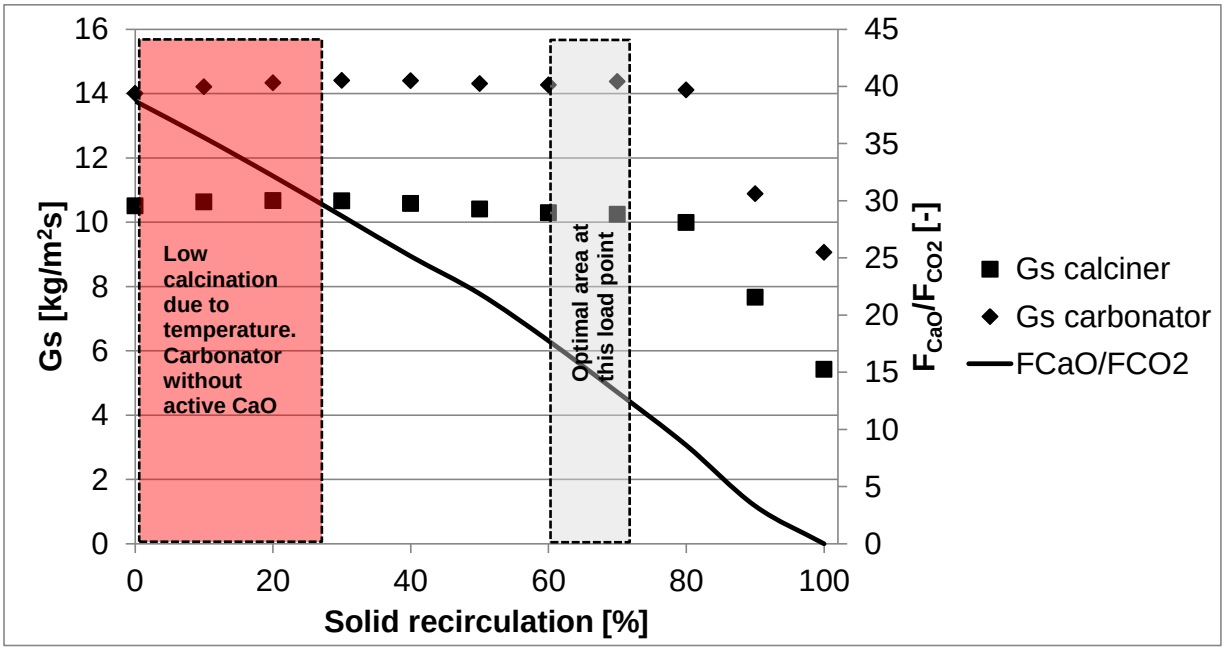
Gs [kg/m²s]
FCaO/FCO2 [-]
Solid recirculation [%]
Low calcination due to temperature. Carbonator without active CaO
Optimal area at this load point
Gs calciner
Gs carbonator
FCaO/FCO2

Table 1.

Fuel property	
Lower heating value [MJ/kg]	29
Proximate analysis [weight-fraction]	
Char	0.56
Volatiles	0.27
Moisture	0.07
Ash	0.10
Ultimate analysis [weight-fraction]	
C	0.794
H	0.041
S	0.016
N	0.009
O	0.140
Average fuel particle diameter [μm]	500
Average fuel density [kg/m^3]	500

Table 2.

Parameter	Carbonator	Calciner
Height [m]	15	15
Diameter [m]	0.65	0.75
Solid inventory [kg]	~450	~350
Gas mass flow [kg/s]	0.35	0.4
Gas O_2 [w-%]	6	40
Gas CO_2 [w-%]	23	60
Gas N_2 [w-%]	63	0
Gas H_2O [w-%]	9	0
Input gas temperature [ºC]	120	50
Fuel flow [kg/s]	-	0.01-0.07
Fuel LHV [MJ/kg]	29	29
Thermal power [MW]	-	0.3-2.0
Average solid diameter [µm]	100	100
Average solid density [kg/m^3]	1800	1800
Carbonator cooling [kW]	0-800	-
Maximum carrying capacity [-]	0.15	0.15
Circulation coefficient of the reactors	0.8	0.8
Recirculation percentage [%]	0-100	0-100